International Journal of Engineering, Mathematical and Physical Sciences
ISSN: 2517-9934
Vol:8, No:3, 2014

Numerical Study on Improving Indoor Thermal Comfort Using a PCM Wall

M. Faraji, F. Berroug

***Abstract*—**A one-dimensional mathematical model was developed in order to analyze and optimize the latent heat storage wall. The governing equations for energy transport were developed by using the enthalpy method and discretized with volume control scheme. The resulting algebraic equations were next solved iteratively by using TDMA algorithm. A series of numerical investigations were conducted in order to examine the effects of the thickness of the PCM layer on the thermal behavior of the proposed heating system. Results are obtained for thermal gain and temperature fluctuation. The charging discharging process was also presented and analyzed.

***Keywords*—**Phase change material, Building, Concrete, Latent heat, Thermal control.

I. Introduction

PHASE CHANGE MATERIALS (PCMs) have been used for thermal storage in buildings since before 1980. In first steps, development and testing were conducted for prototypes of PCM wallboard and PCM concrete systems to enhance the thermal energy storage capacity of standard wallboard and concrete blocks, with particular interest in peak load shifting and solar energy utilization [1]-[3]. In building-integrated applications, PCMs have been incorporated into gypsum wallboards to provide passive energy storage. Several authors investigated the various methods for impregnating gypsum and other PCMs in wallboards [4]-[6]. Zalba et al. [7] studied building-integrated phase change material. Parametric simulations of the thermal performance of the wall were performed to account for the influences of external and internal ambient environments, daily solar radiation, and thickness as well as the melting point of the PCM layer. The results show that, incorporating the appropriate phase change material layer can improve the thermal performances of the wall. Zhang et al. [8] presented the development of a thermally enhanced wall that reduces peak air-conditioning demand in residential buildings. Berroug et al. [9] analyzed the thermal performance of a north wall made with hydrate salt phase change material as a storage medium in east-west oriented greenhouse. A numerical study has been developed to investigate the impact of the PCM on greenhouse temperature. Results show that, with an equivalent to 32.4kg of PCM per square meter of the greenhouse area, temperature of inside air were found to be 6°C more at night in winter period with less fluctuations.

M. Faraji is with Hassan II University, Faculty of Sciences AinChock, Physics Department- LPMMAT Laboratory, PO 5366 Maarif, Casablanca-Morocco (corresponding author to provide phone: +212-631-756-990; e-mail: farajimustapha@yahoo.fr).

F. Berroug is with Cadi Ayyad University, Laboratoire d'Automatique de l'Environnement et Procédés de Transfert, Faculté des Sciences Semlalia-Département de Physique, Marrakech- Morocco (e-mail: f.berroug@uca.ma).

II. Mathematical Model

Fig. 1 shows the physical system studied in the present work. It consists of a sandwiched wall made with three layers. The outside and the inside layers are concrete, the medium is PCM. The total thickness of the wall is L=20cm and the PCM layer is located near to the inner face at constant position x_m. The thickness of the PCM layer is e_m=0.5cm. The wall corresponding thermal properties are given in Table I. The composite PCM wall was initially at a uniform temperature, T_{ini}=16°C. The boundary conditions on the outer surface of wall are due to the combined effects of solar radiation and ambient air convection. Typical Mediterranean meteorological data for every one hour during January are used (Fig. 2).

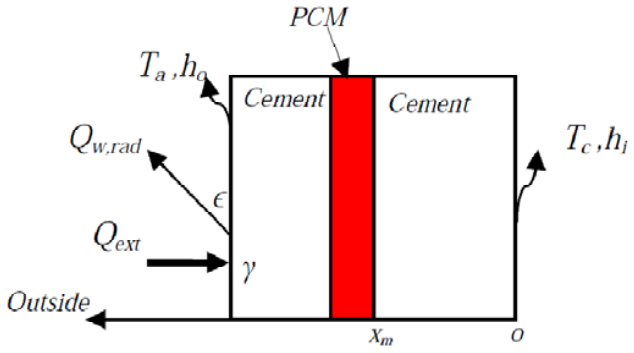

Fig. 1 Physical model

Some assumptions were made in order to simplify its resolution. These assumptions are given as follows:

- thermal properties are constant and not varying with respect to temperature;
- end effects are neglected;
- interfacial resistances are negligible;
- heat transfer through the wall is assumed 1 D ;
- buoyancy induced flow in the melt PCM is neglected.

The energy transport in PCM/wall may be written using the enthalpy formulation [10]:

$$\partial H/\partial t = \nabla(\mathrm{k}\nabla\mathrm{T}) \quad (1)$$

where,

$$H(T) = h(T) + \rho\,\lambda\ \ f\Delta H_f \quad (2)$$

and

$$h(T) = h(T_m) + \int_{T_m}^{T} \rho c_p \, dT \quad (3)$$

λ =1 in PCM and λ =0 in concrete layers.

Using sensible enthalpy h, (1) is rewritten as:

$$\frac{\partial h}{\partial t} = \alpha \frac{\partial^2 h}{\partial x^2} - \rho \lambda \Delta H_f \frac{\partial f}{\partial t} \quad (4)$$

The liquid fraction f in the PCM layer is estimated as:

$$f = \begin{cases} 1 \text{ for } T > T_m \\ 0 \text{ for } T < T_m \\ 0 < f < 1 \text{ for } T = T_m \end{cases} \quad (5)$$

The continuity of the temperature and heat flux density are used at the interfaces concrete/PCM. The thermal properties at interfaces were obtained by the following relations:

$$k_i = \frac{k_+ k_- (\delta_- + \delta_+)}{k_+ \delta_- + k_- \delta_+}, \; k_m = f k_l + (1-f) k_s, \quad \rho c_p = f (\rho c_p)_l + (1-f) (\rho c_p)_s \quad (6)$$

where δ_- is the distance between the interface and the first node inside the PCM region and δ_+ is the distance between the interface and the first node inside the concrete layer. The boundary conditions are as follows:

- at x=0:

$$-k \frac{\partial T}{\partial x}\Big|_{x=0} = h_i (T_c - T) \quad (7)$$

- at $x=L$:

$$-k \frac{\partial T}{\partial x}\Big|_{x=L} = h_o (T_a - T) + Q_{w,rad} + \gamma Q_{ext} \quad (8)$$

where,

$$Q_{w,rad} = \sigma \varepsilon F (T_{sky}^4 - T^4) = h_{sky}^r (T_a - T) \quad (9)$$

here, the sky is considered as black body at T_{sky} (°C) [11]:

$$T_{sky} = 0.0552 \times (T_a + 273.16)^{1.5} - 273.16 \quad (10)$$

The irradiative heat transfer coefficient h_{sky}^r is given by:

$$h_{sky}^r = \frac{\sigma \varepsilon (T_{sky}^4 - T^4)}{T_a - T} \quad (11)$$

The shape factor F is assumed to be equal to one.

- Heat flux at interfaces, $x = x_m$ and $x = x_m + e_m$, between PCM and concrete is evaluated as:

$$q_i'' \approx \frac{k_+ k_-}{k_+ \delta_- + k_- \delta_+} (T_+ - T_-) \quad (12)$$

TABLE I
THERMOPHYSICAL PROPERTIES [1]

Material	Organic PCM	Concrete
T_m (°C)	22	-
ΔH_f (kJ/kg)	148.5	-
ρ (kg/m^3)	981 (Solid) 862 (Liquid)	2200
k (W/mK)	0. 415	1.5
c_p (J/kg K)	1460 (Solid) 2130 (Liquid)	838
γ	-	0.9
ε	-	0.85

Herein, natural convection heat transfer coefficients considered are: h_i =5 W/mK and h_o=20 W/mK.

The governing equations were integrated using finite volume technique [12]. It should be noted that the obtained equations are non linear because the irradiative transfer coefficient, h_{sky}^r, can appear with the term, T^4, in the irradiative component. To resolve this problem iteratively, the above terms must be considered constant within each time step. The new value of the obtained temperature will be used in none linear irradiative heat transfer coefficient.

The convergence of the calculus was declared, at each time step, when a criterion based on the energy conservation principle was satisfied. A grid and time step refinement was carried out and showed that the time step of 60 s and a size grid of 50 nodes were found to be adequate for all the computations. A self-Fortran computer code was developed in order to implement the above numerical method.

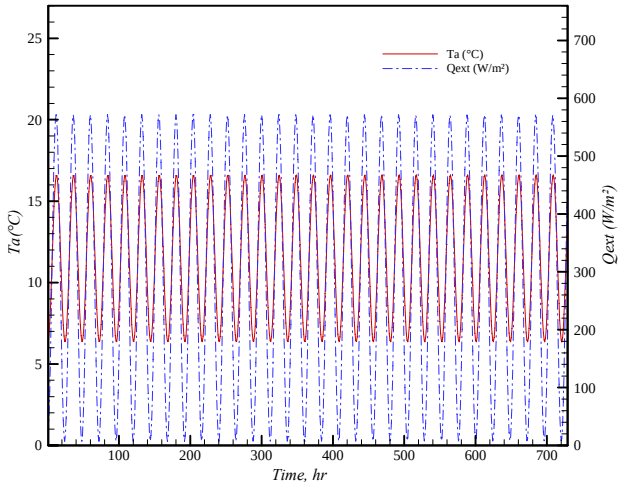

Fig. 2 Time wise variations of the ambient temperature, T_a, and the global solar radiations, Q_{ext}, received by a south oriented vertical wall

III. Result and Discussion

Fig. 2 shows the time wise variation of the ambient temperature, T_a, during typical days representing the cold period of the year (winter -January in Mediterranean zones). Ambient temperature rises due to the sunrise and falls during the night. This oscillatory phenomenon (increase followed by a decrease) is due to the alternating day/night every 24 hours.

The minimum temperatures are obtained during the night. On average, temperatures minima and maxima range between 6°C and 18°C, respectively, and the ambient temperature swing between these extremes. Fig. 2 shows also the evolution of the global solar radiations, Q_{ext}, received by a south oriented vertical wall for typical days during January. The radiation increases with the sunrise which causes the ambient temperature increase. Solar radiation reaches a maximum value (600 W/m²) between solar noon and 15h00 and vanishes at 18h00 which present the sunset. Mediterranean zones climate are characterized by severe temperature fluctuations during winter and lower values of temperature are reached.

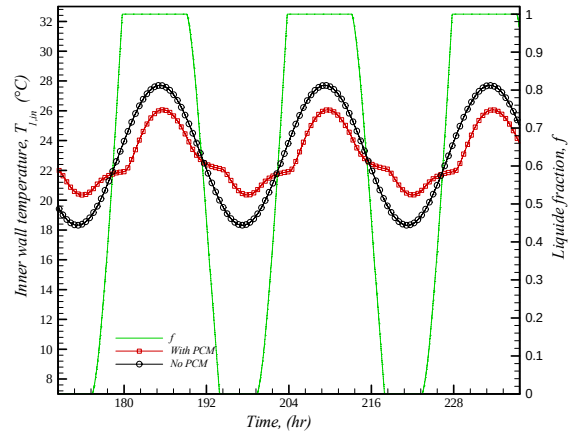

(a)

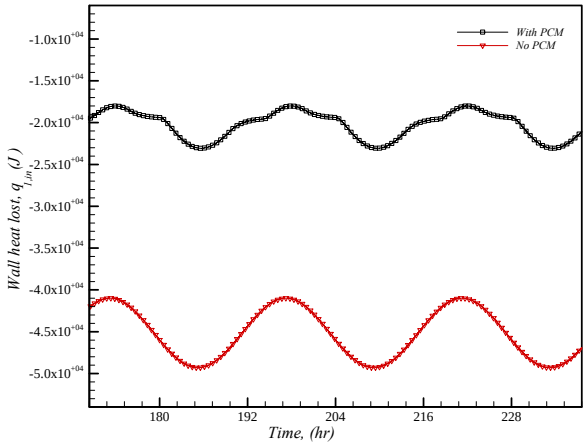

(b)

Fig. 3 Comparison of the inner wall temperature, $T_{1,in}$, (a) and heat lost, $q_{1,in}$, (b)

Fig. 3 (a) compares the thermal behavior of an ordinary wall and the composite wall with PCM, T_m=22°C (Table I). The PCM layer is located at fixed position x_m=1.5cm. Data analysis shows that the inside wall temperature increases from 21°C to 25°C and from 18°C to 28°C, for wall/PCM and an ordinary concrete wall, respectively. The ambient temperature increases between 7°C to 18°C (Fig. 2) and the PCM layer receives also a heat flux due to the solar radiations absorbed by the concrete (γ =0.8) combined with convective heat flux that increases the PCM temperature to the melting point (T_m= 22°C). Remind that, during melting process, sensible heat storage stops and the latent heat storage develops with fusion process: latent heat storage starts and, as a result, a first layer of the liquid phase appears (f > 0). For the PCM wall case, the slop of temperature curve weakens during the phase change process because melting and solidification occur at constant temperature. The increase of solar radiation accumulates sensible heat storage in concrete and latent heat in PCM layer. The composite wall can be considered as an important storage device. The excess of heat is stored in the wall with less temperature variation until the full melting of PCM (f=1). The stored heat during a day is used for heating needs in the following night.

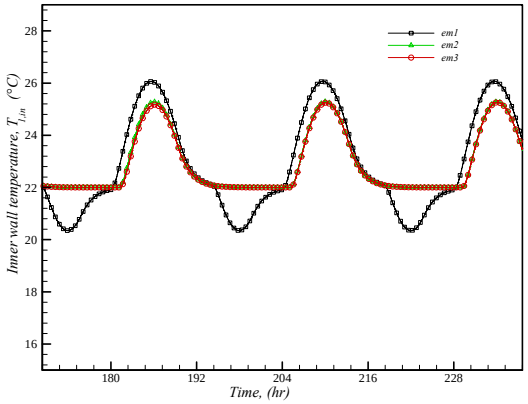

(a)

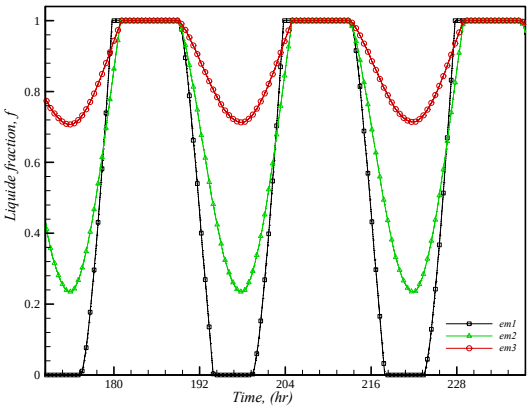

(b)

Fig. 4 Variation of the concrete/PCM wall temperature (a) and liquid fraction (b) for different PCM thicknesses e_m

Fig. 3 (a) shows also that, the ambient temperature decreases after reaching a maximum. Liquid fraction increases until PCM becomes totally melted (f=1). Note that the sensible heating continues and leads to the increase of the outer wall face temperature. The overheating of the liquid

PCM layer is due to the raise of the sensible heat storage during that period and, therefore, leads to the increase of the wall temperature. This process continues until the decrease of liquid fraction. The discharging process activates at sunset and the inner wall temperature falls after a certain delay due to the thermal inertia and to the weak value of its thermal conductivity. Note that minimum temperature reached in case of the wall with PCM is clearly greater than that achieved without PCM because the shrink of the wall temperature is shifted by the use of the important stored latent heat.

Fig. 3 (b) represents the thermal gradients, $q_{1,in}$, occurring between the inner face and indoor air for wall with and without PCM. Theses values quantify the thermal lost. Analysis of such figure confirms the above results. Thermal gradient, in the case with PCM, is less than that without PCM. For wall without PCM, thermal gradients alternate between -50kJ and -40kJ and temperature fluctuations are clearly more pronounced. The inner wall loses the heat. The PCM wall achieves more efficient in thermal insulation and increases the thermal efficiency of the building during the coldest period of the year.

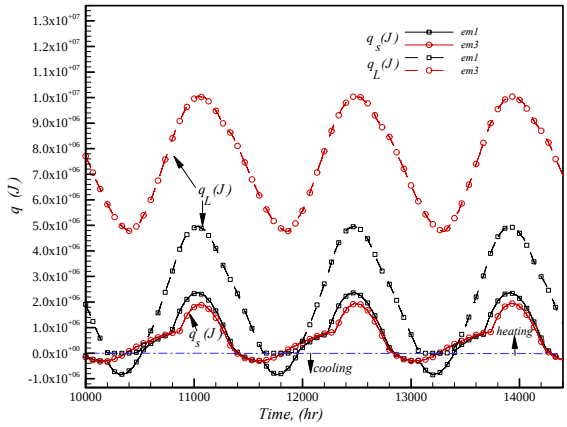

Fig. 5 Latent and sensible heat storage for different PCM thicknesses e_m

In order to investigate the effect of the PCM quantity on the thermal performance of the wall, a study was conducted by modifying the thicknesses of the PCM layer, e_m, then examining its effect on, $T_{1,in}$, f, q_s , q_L and temperature swings. Fig. 4 sketches the time wise variation of the concrete/PCM wall temperature and liquid fraction for different values of e_m (e_{m1} =0.5cm, e_{m2} = 1cm and e_{m3} =3cm). Data analysis of such a figure shows that when the PCM layer thick is superior to 1 cm better are the living thermal conditions with less temperature fluctuations. For the lower value of e_m PCM completely solidify at night (f =0, Fig. 4 (b)). For all cases, PCM remains in liquid state during about 8 hours during each day and that implements the liquid phase to become superheated. In fact, sensible heat q_s increases during that period as illustrated in Fig. 5. The de-emphasis between Q_{ext} and T_a and the wall thermal inertia leads to the delayed maxima for the inner temperatures as illustrated by Fig. 4 (a). For higher PCM quantity, phase change material doesn't completely solidify and latent heat stored in the day is note completely used during the night. This result is confirmed also by Fig. 5 where latent heat q_L remains greater than zero during the night for e_{m2}.

IV. Conclusion

A south wall incorporating a phase change material was modeled using the enthalpy method. The thermal performances of the proposed composite wall, used for heating application, were monitored under typical working conditions. It was emerged that the PCM/concrete wall is able to provide good performance. The PCM layer thick must be sufficient to give better living thermal conditions with less inner temperature fluctuations.

Nomenclature

c_p	specific heat, (kJ/kg K)
f	liquid fraction
e_m	PCM layer thickness, (m)
H	enthalpy, (J)
h	convective heat transfer coefficient, (W/m^2 K)
h^r_{sky}	irradiative heat transfer coefficient, (W/m^2 K)
k	thermal conductivity, (W/m K)
L	total wall thickness, (m)
$q_{1,in}$	heat lost per square meter of the inner wall, (J)
q_S	sensible heat stored per square meter of the wall , (J)
Q_{ext}	solar radiation, (W/m2)
$Q_{w,rad}$	heat lost to the ambient by radiations, (J)
t	time, (s)
T	temperature, (°C)
Indices	
in	inner face
m	melting, PCM
c	comfort
sky	sky
out	outer wall face
+,-	right, left nodes
f	fusion
Greeks	
ρ	density, (kg/m^3)
γ	absorptivity
α	thermal diffusivity, (m/s^2)
σ	Stefan Boltzmann constant
ε	concrete emissivity
ΔH_f	latent heat of PCM (kJ/kg)

References

[1] B. Zalba, J.M. Marín, L.F Cabeza, Mehling H. Review on thermal energy storage with phase change: materials, heat transfer analysis and applications. Applied Thermal Engineering; 23:251e83, 2003.

[2] M. Faraji, Numerical computation of solar heat storage in phase change material/concrete wall. International Journal of Energy and Environment, vol 5, (3).353-360 ,2014.

[3] Li. B. Z, Zhang C.L, Deng A. Study on improving indoor thermal environment in light weight building combining PCM wall and nighttime ventilation. Journal of Civil Architectural & environmental Engineering 31(3) 2009.

[4] J.Paris, Villain, J.-F Houle. Incorporation of PCM in wallboards: a review of recent developments. In: Proceedings of the First World Renewable Energy Congress, September, Reading, UK, pp. 2397–2401, 1990.

[5] K. Peippo, P. Kauranen, P.D. Lund, A multicomponent PCM wall optimized for passive solar heating, Energy and Buildings 17 259–270

(1991).
[6] D.A. Neeper, Thermal dynamics of wall board with latent heat storage, Solar Energy 68 393–403 (2000).
[7] B. Zalba, J. M. Marın, L. F. Cabeza, H. Mehling, Free-cooling of buildings with phase change materials, International Journal of Refrigeration 27 839–849 (2004).
[8] M. Zhang, A.M. Medina, B.J. King, Development of a thermally enhanced frame wall with phase change materials for on-peak air-conditioning demand reduction and energy + savings in residential buildings, International Journal of Energy Research, Green heck Fan Corporation, Schofield, WI, U.S.A (2005).
[9] F. Berroug, E.K. Lakhal, M. El Omari, M. Faraji, H. El Qarnia, Thermal performance of a greenhouse with a phase change material north wall, Energy and Buildings 43 3027–3035 (2011).
[10] V.R. Voller and S.Peng An enthalpy formulation based on an arbitrarily mesh for solution of the stefan problem. Computational Mechanics, 14:492-502, 1994.
[11] W.C. Swinbank, Long-Wave radiation from clearskies, Quarterly Journal of the Royal Meteorological Society 381(89) 339-348, (1963).
[12] Patankar, S.V., Numerical Heat Transfer and Fluid Flow, Hemisphere, 1983.